

# Genomic Evidence for Hybridization and Introgression in a North American Toad (*Anaxyrus*) Hybrid Zone

Kerry A. Cobb<sup>\*1</sup> and Jamie R. Oaks<sup>2</sup>

<sup>1</sup>Department of Biological Sciences, Mississippi State University,  
Mississippi State, MS 39762

<sup>2</sup>Department of Biological Sciences & Museum of Natural History, Auburn  
University, 101 Rouse Life Sciences Building, Auburn, Alabama 36849

August 2, 2024

## 1 Abstract

Hybrid zones present an excellent opportunity to study the evolution of reproductive isolation between divergent evolutionary lineages as generations of interbreeding and backcrossing produce many different recombinant genotypes. We can then observe patterns of genetic variation within a hybrid zone to understand how selection is acting on these recombinant genotypes. Using genome-wide sequence data, we characterized patterns of introgression within a putative hybrid zone between two species of North American toads (*A. americanus* and *A. terrestris*) to better understand reproductive isolation between these species. Both model based and non-parametric approaches to population

---

<sup>\*</sup>(Corresponding author: [cobbkerry@gmail.com](mailto:cobbkerry@gmail.com))

structure inference showed that there is likely a substantial level of interbreeding and successful backcrossing at this hybrid zone with admixed individuals located quite far from the center of the hybrid zone. Bayesian genomic cline analysis revealed loci with extreme patterns of introgression relative to other loci which would be expected if these sites were linked to sites under negative selection in a hybrid genomic background. A site-based measure of genetic divergence was found to be weakly correlated with cline parameter estimates. We argue that this weak correlation is consistent with a history of secondary contact following a period of geographic isolation as many highly divergent sites do not have correspondingly high cline parameter estimates consistent with strong selection against introgression. Our findings substantiate previous claims of the existence of a hybrid zone between *A. americanus* and *A. terrestris* and highlight the potential for this hybrid zone to further our understanding of the evolution of reproductive incompatibility.

## 2 Introduction

The evolution of reproductive isolation between divergent lineages is a continuous process during which there may be ongoing gene flow or introgression via hybridization (Mallet, 2008; Wu, 2001). Introgression is possible because genetic barriers to introgression that accumulate within the genome are a property of genomic regions rather than a property of the entirety of the genome (Gompert, Parchman, et al., 2012; Wu, 2001). Natural hybridization between divergent lineages has become increasingly appreciated as a widespread phenomenon in recent years (Mallet, 2005; Moran et al., 2021). It is a phenomenon that can have important evolutionary consequences. Hybridization can be a source of adaptive variation (Hedrick, 2013). It can also introduce deleterious genetic load which persists long term within a population (Moran et al., 2021). Hybridization can potentially create conditions where selection favors the evolution of traits that enhance assortative mating and reduce the production of unfit hybrid offspring which drives further genetic divergence and reinforcement of reproductive barriers between lineages (Servedio

& Noor, 2003). If hybrids do not suffer any negative fitness effects, hybridization could lead to the erosion of differences between divergent populations (Taylor et al., 2006), potentially resulting in populations that are genetically distinct from either parent species which can themselves eventually evolve reproductive isolation from the parent species (Moran et al., 2021).

Aside from having important evolutionary consequences which need to be understood, hybridization provides an excellent opportunity to investigate the processes that result in the evolution of reproductive incompatibility and divergence between evolutionary lineages. Hybrid zones are particularly suitable for this due to the production of a large number of recombinant genomes carrying many possible combinations of genomic elements from parent species resulting from generations of backcrossing (Rieseberg et al., 1999). Many generations of backcrossing and recombination make it possible to distinguish between the effects of closely linked genes (Rieseberg et al., 1999), and it is not feasible to achieve this experimentally in the vast majority of species (Rieseberg et al., 1999). Furthermore, the combination of genes produced are exposed to selection under natural conditions. This is important as the effect of hybrid incompatibilities can be dependent on environmental conditions and can only be fully understood in this context (Miller & Matute, 2016).

Despite being a fundamental evolutionary process, our understanding of evolution of reproductive incompatibility is far from complete (Butlin et al., 2011). Only a few loci, in a few species, have been pinpointed as the direct cause of reproductive incompatibility between species (Blackman, 2016; Nosil & Schlüter, 2011). Consequently, our understanding of the processes that drive the evolution of loci resulting in reproductive incompatibility is limited (Butlin et al., 2011). Studies of introgression within hybrid zones have identified highly variable rates of introgression among loci (Barton & Hewitt, 1985; Gompert et al., 2017). This heterogeneity can arise via genetic drift occurring within hybrid zones, but will also be caused by differences among loci in the strength of selection against them in a hybrid genomic background (Barton & Hewitt, 1985; Gompert et al., 2017). It has also been observed that the levels of genetic divergence between

species are highly variable across the genome (Nosil et al., 2009). Much of this heterogeneity is the result of divergent selection acting on each species independently (Nosil et al., 2009). Regions with particularly high levels of divergence between closely related species have been coined "genomic islands of divergence" (Wolf & Ellegren, 2017). It is assumed, particularly in the case of speciation with gene flow, that these genomic islands harbor genes that reduce the likelihood of successful interbreeding between species. When speciation occurs with gene flow, divergent selection can cause adaptive divergence in habitat use, phenology, or mating signals, and reduce the frequency or success of interspecific matings (Coyne & Orr, 2004). When species diverge in geographic isolation, divergent selection and reproductive isolation could be decoupled and reproductive isolation is not the result of direct selection against interspecific matings. Whether loci under divergent selection between two species also contribute to reproductive isolation has not been widely explored. A handful of studies have found evidence for a modest relationship between genetic divergence and selection against introgression (Gompert, Lucas, et al., 2012; Larson et al., 2013; Nikolakis et al., 2022; Parchman et al., 2013). How consistent and widespread this pattern is remains to be seen. At least one study published by Jahner et al. (2021) found no association.

In this study, we investigate hybridization between the American toad (*Anaxyrus americanus*) and Southern toad (*Anaxyrus terrestris*) at a suspected hybrid zone in the Southern United States to assess the extent of introgression between them and test for a relationship between introgression and genetic divergence. This suspected hybrid zone has not been investigated with genetic data previously, but it bears many hallmarks of a tension zone (Barton & Hewitt, 1985). Under the tension zone model of hybridization, species boundaries are maintained by a balance between dispersal and selection against individuals carrying incompatible hybrid genotypes (Barton & Hewitt, 1985). The ranges of *A. americanus* and *A. terrestris* abut with an abrupt transition and no apparent overlap along a long contact zone which ranges from Louisiana to Virginia. This contact zone closely corresponds with a prominent physiographic feature known as the "fall line" (Mount, 1975; Powell et al., 2016). The Fall line is the boundary between the Southern

coastal plain to the South and the Appalachian Highlands to the North (Shankman & Hart, 2007). These regions differ in their underlying geology, topography, and elevation (Shankman & Hart, 2007). The distribution of *A. terrestris* is restricted to the coastal plain extending from the Mississippi River in the West to Virginia in the East (Fig. 1). The distribution of the American Toad encompasses nearly all of the Eastern North American with the exception of the Southern coastal plain (Fig. 1). Tension zones are expected to correspond with natural features that reduce dispersal or abundance and such a sudden transition is difficult to explain if not the result of the processes characteristic of tension zones (Barton, 1979). For there to be no mutually hospitable areas permitting some range overlap is implausible without there being an extreme level of competition or extreme degree of adaptation by each species to their respective environments. The two species only differ slightly in male advertisement call, morphological appearance, and the timing of their spawn (Cocroft & Ryan, 1995; Mount, 1975; Weatherby, 1982). Although there is some overlap in the spawning period and male Bufonidae are famously indiscriminate in their choice of mates (Đorđević & Simović, 2014; Weatherby, 1982). They have also been shown to have a degree of reproductive compatibility through laboratory crossing experiments which produced viable  $F_2$  offspring (Blair, 1963). Analysis of morphological variation in central Alabama by Weatherby (1982) suggests there has been introgression between them.

The "true toads" in the family Bufonidae, to which *A. americanus* and *A. terrestris* belong, have been a prominent group of organisms in the literature on hybridization. W.F. Blair and colleagues performed a remarkable 1,934 separate experimental crosses to quantify the degree of reproductive incompatibility between species pairs within this family (Blair, 1972; Malone & Fontenot, 2008). These experiments demonstrated a high degree of compatibility between some closely related species pairs in which hybrids were capable of producing viable backcross or  $F_2$  hybrid offspring (Blair, 1963). Furthermore, numerous cases of natural hybridization among toad species have been reported with several apparent as well as indisputable hybrid zones (Colliard et al., 2010; Green, 1996; Van Riemsdijk et al., 2023; Weatherby, 1982). Despite the interest in and appreciation

for hybridization in Bufonidae, only a small amount of work has been done to understand patterns of introgression within Bufonid hybrid zones. Just three hybrid zones have been investigated using genetic data. A clinal pattern of admixture at 26 allozyme loci has been shown within the *Anaxyrus americanus* X *Anaxyrus hemiophrys* hybrid zone in Ontario, Canada (Green, 1983). Almost no admixture was detected at 7 microsatellite loci within the suspected *Bufo siculus* X *Bufo balearicus* hybrid zone in Sicily, Italy (Colliard et al., 2010). The most comprehensive study of introgression within a Bufonidae hybrid zone found significant levels of genome wide admixture, fitting a clinal pattern, at two separate transects at either end of the *Bufo bufo* x *Bufo spinosus* hybrid zone in Southern France (Van Riemsdijk et al., 2023).

The suspected *A. americanus*, *A. terrestris* hybrid zone has great potential to expand our understanding of the evolution of reproductive incompatibility. However, this will be dependent on the degree of ongoing introgression, if any, between these species. In this study, we use genome-wide sequence data to characterize patterns of introgression within the hybrid zone using model-based inference of admixture proportions, Bayesian genomic cline analysis, and estimates of parental population differentiation. With these approaches, we specifically address the following questions: 1) Is there evidence of ongoing hybridization and admixture between the two species, 2) Do any loci have outstanding patterns of introgression consistent with them being linked to reproductive incompatibility, and 3) Is there any relationship between patterns of introgression and levels of genetic differentiation between parental lineages?

## 3 Methods

### 3.1 Sampling and DNA Isolation

We collected genetic samples from *A. americanus* and *A. terrestris* by driving roads during rainy nights between 2017 and 2020 in a region of central Alabama where hybridization has previously been inferred from the presence of morphological intermediate individuals (Weatherby, 1982). For each individual collected, we euthanized it with

immersion in buffered MS-222, preserved genetic samples of liver and/or toes in 100% ethanol, and preserved the rest of the specimen with 10% buffered formalin solution.

We euthanized individuals with immersion in buffered MS-222. We removed liver and/or toes and preserved them in 100% ethanol and fixed specimens with 10% Formalin solution. Genetic samples and formalin fixed specimens were deposited at the Auburn Museum of Natural History. Additional samples were also provided by museums (see Table S2).

We isolated DNA by lysing a small piece of liver or toe approximately the size of a grain of rice in a 300  $\mu$ L solution of 10mM Tris-HCL, 10mM EDTA, 1% SDS (w/v), and nuclease free water along with 6 mg Proteinase K and incubating for 4-16 hours at 55°C. To purify the DNA and separate it from the lysis product, we mixed the lysis product with a 2X volume of SPRI bead solution containing 1 mM EDTA, 10 mM Tris-HCl, 1 M NaCl, 0.275% Tween-20 (v/v), 18% PEG 8000 (w/v), 2% Sera-Mag SpeedBeads (GE Healthcare PN 65152105050250) (v/v), and nuclease free water. We then incubated the samples at room temperature for 5 minutes, placed the beads on a magnetic rack, and discarded the supernatant once the beads had collected on the side of the tube. We then performed two ethanol washes by adding 1 mL of 70% ETOH to the beads while still placed in the magnet stand and allowing it to stand for 5 minutes before removing and discarding the ethanol. After removing all ethanol from the second wash, we removed the tube from the magnet stand and allowed the sample to dry for 1 minute before thoroughly mixing the beads with 100  $\mu$ L of TLE solution containing 10 mM Tris-HCL, 0.1 mM EDTA, and nuclease free water. After allowing the bead mixture to stand at room temperature for 5 minutes, we returned the beads to the magnet stand, collected the TLE solution, and discarded the beads. We quantified DNA in the TLE solution with a Qubit fluorometer (Life Technologies, USA) and diluted samples with additional TLE solution to bring the concentration to 20 ng/ $\mu$ L.

### 3.2 RADseq Library Preparation

We prepared RADseq libraries using a the 2RAD approach developed by Bayona-Vásquez et al. (2019) with some minor modifications. On 96 well plates, we ligated 100 ng of sample DNA in 15  $\mu$ L of a solution with 1X CutSmart Buffer (New England Biolabs, USA; NEB), 10 units of XbaI, 10 units of EcoRI, 0.33  $\mu$ M XbaI compatible adapter, 0.33  $\mu$ M EcoRI compatible adapter, and nuclease free water with a 1 hour incubation at 37°C. We then immediately added 5  $\mu$ L of a solution with 1X Ligase Buffer (NEB), 0.75 mM ATP (NEB), 100 units DNA Ligase (NEB), and nuclease free water and incubated at 22°C for 20 min and 37°C for 10 min for two cycles, followed by 80°C for 20 min to stop enzyme activity. For each 96 well plate, we pooled 10  $\mu$ L of each sample and split this pool equally between two microcentrifuge tubes. we purified each pool of libraries with a 1X volume of SpeedBead solution followed by two ethanol washes as described in the previous section except that the DNA was resuspended in 25  $\mu$ L of TLE solution and combined the two pools of cleaned ligation product.

In order to be able to detect and remove PCR duplicates, we performed a single cycle of PCR with the iTru5-8N primer which adds a random 8 nucleotide barcode to each library construct. For each plate, we prepared four PCR reactions with a total volume of 50  $\mu$ L containing 1X Kapa Hifi Buffer (Kapa Biosystems, USA; Kapa), 0.3  $\mu$ M iTru5-8N Primer, 0.3 mM dNTP, 1 unit Kapa HiFi DNA Polymerase, 10  $\mu$ L of purified ligation product, and nuclease free water. We ran reactions through a single cycle of PCR on a thermocycler at 98°C for 2 min, 60°C for 30 s, and 72°C for 5 min. We pooled all of the PCR products for a plate into a single tube and purified the libraries with a 2X volume of SpeedBead solution as described above and resuspended in 25  $\mu$ L TLE. We added the remaining adapter and index sequences which were unique to each plate with four PCR reactions with a total volume of 50  $\mu$ L containing 1X Kapa Hifi (Kapa), 0.3  $\mu$ M iTru7 Primer, 0.3  $\mu$ M P5 Primer, 0.3 mM dNTP, 1 unit of Kapa Hifi DNA Polymerase (Kapa), 10  $\mu$ L purified iTru5-8N PCR product, and nuclease free water. We ran reactions on a thermocycler with an initial denaturation at 98°C for 2 min, followed by 6 cycles of 98°C for 20 s, 60°C for 15 s, 72°C for 30 s and a final extension of 72°C for 5 min. We pooled

all of the PCR products for a plate into a single tube and purified the product with a 2X volume of SpeedBead solution as described above and resuspended in 45  $\mu$ L TLE.

We size selected the library DNA from each plate in the range of 450-650 base pairs using a BluePippin (Sage Science, USA) with a 1.5% dye free gel with internal R2 standards. To increase the final DNA concentrations, we prepared four PCR reactions for each plate with 1X Kapa Hifi (Kapa), 0.3  $\mu$ M P5 Primer, 0.3  $\mu$ M P7 Primer, 0.3 mM dNTP, 1 unit of Kapa HiFi DNA Polymerase (Kapa), 10  $\mu$ L size selected DNA, and nuclease free water and used the same thermocycling conditions as the previous (P5-iTru7) amplification. We pooled all of the PCR products for a plate into a single tube and purified the product with a 2X volume of SpeedBead solution as before and resuspended in 20  $\mu$ L TLE. We quantified the DNA concentration for each plate with a Qubit fluorometer (Life Technologies, USA) then pooled each plate in equimolar amounts relative to the number of samples on the plate and diluted the pooled DNA to 5 nM with TLE solution. The pooled libraries were pooled with other projects and sequenced on an Illumina HiSeqX by Novogene (China) to obtain paired-end, 150 base-pair sequences.

### 3.3 Data Processing

We demultiplexed the iTru7 indexes using the *process\_radtags* command from *Stacks* v2.6.4 (Rochette et al., 2019) and allowed for two mismatches for rescuing reads. To remove PCR duplicates, we used the *clone\_filter* command from *Stacks*. We demultiplexed inline sample barcodes, trimmed adapter sequence, and filtered reads with low quality scores as well as reads with any uncalled bases using the *process\_radtags* command again and allowed for the rescue of restriction site sequence as well as barcodes with up to two mismatches. We built alignments from the processed reads using the *Stacks* pipeline. We allowed for 14 mismatches between alleles within, as well as between individuals (M and n parameters). This is equivalent to a sequence similarity threshold of 90% for the 140 bp length of reads post trimming. We also allowed for up to 7 gaps between alleles within and between individuals. We used the *populations* command from *Stacks* to filter loci missing in more than 5% of individuals, filter all sites with minor allele counts less

than 3, filter any individuals with more than 90% missing loci, and to randomly sample a single SNP from each locus.

### 3.4 Genetic Clustering & Ancestry Proportions

To cluster individuals and characterize patterns of genetic differentiation and admixture between clusters, I used the Bayesian inference program *STRUCTURE* v2.3.4 (Pritchard et al., 2000) with *STRUCTURE*'s admixture model which returns an estimate of ancestry proportions for each sample. To evaluate the assumption that samples are best modeled as inheriting their genetic variation from the two groups corresponding to the species identification made in the field, we ran *STRUCTURE* under four different models, each with a different number of assumed clusters of individuals ( $K$  parameter) ranging from 1 to 4. For each value of  $K$ , we ran 20 independent runs for 100,000 total steps with the first 50,000 as burnin. We used the R package *POPHELPER* v2.3.1 (Francis, 2017) to combine iterations for each value of  $K$  and to select the model producing the largest  $\Delta K$  which is the the model that has the greatest increase in likelihood score from the model with one fewer populations as described by (Evanno et al., 2005). We also examined genetic clustering and evidence of admixture using a non-parametric approach with a principal component analysis (PCA) implemented in the R package *adegenet* v2.1.10 (Jombart, 2008). We visualized the relationship between the first principal component axis and the model based estimates of admixture proportion for each individual to check for agreement between the parametric *STRUCTURE* analysis and the non-parametric PCA analysis.

### 3.5 Genomic Cline Analysis

To investigate patterns of introgression across the hybrid zone we used the Bayesian genomic cline inference tool *BGC* v1.03 (Gompert & Buerkle, 2012) to infer parameters under a genomic cline model. A genomic cline model has two key parameters, denoted  $\alpha$  and  $\beta$ , which describe introgression at each locus based on the estimated ancestry proportion or hybrid index of individuals. The  $\alpha$  parameter is referred to as the cline

center which is the increase (positive value) or decrease (negative value) in the probability of ancestry from one species for a given locus. The  $\beta$  parameter affects the cline rate which is the rate of transition from a low probability to a high probability of ancestry for one species at a given locus. We classified a sample as being admixed for the *BGC* analysis if it had an inferred admixture proportion of <95% for one species under the model with a  $K$  of two in the *STRUCTURE* analysis. We used *VCFtools* v0.1.17 to remove all non-biallelic sites from the the VCF file produced by the *populations* command in *Stacks*. We converted the VCF formatted data into the *BGC* format using *bgc\_utils* v0.1.0, a *Python* package that we developed for this project ([github.com/kerrycobb/bgc\\_utils](https://github.com/kerrycobb/bgc_utils)). We ran *BGC* with 5 independent chains, each for 1,000,000 steps and sampled every 1000. We visualized MCMC output to confirm patterns consistent with the chains converging on a shared stationary distribution, discarded burnin samples, combined the independent chains, and identified outlier loci with *bgc\_utils*.

The primary goal of *BGC* analysis is to identify loci which have exceptional patterns of introgression. These loci, or loci in close linkage to them, are expected to be enriched for genetic regions affected by selection due to reproductive incompatibility between the two species. We identified loci with exceptional patterns of introgression using two approaches described by Gompert and Buerkle (2011). (1) If locus-specific introgression differed from the genome-wide average, which we will refer to as "excess ancestry" following Gompert and Buerkle (2011). More specifically, we classified a locus as having excess ancestry if the 90% highest posterior density interval (HPDI) for the alpha or beta parameter did not cover zero. (2) If locus-specific introgression is statistically unlikely relative to the genome-wide distribution of locus-specific introgression, which we refer to as "outliers" following Gompert and Buerkle (2011). We classified a locus as an outlier if the median of the posterior sample for the  $\alpha$  or  $\beta$  parameters for a locus was not contained in the interval from 0.05 to 0.95 of the cumulative probability density functions  $Normal(0, \tau_\alpha)$  or  $Normal(0, \tau_\beta)$  respectively, where  $\tau_\alpha$  and  $\tau_\beta$  are the median values from the posterior sample for the conditional random effect priors on  $\tau_\alpha$  and  $\tau_\beta$ . These conditional priors describe the genome-wide variation of locus-specific  $\alpha$  and  $\beta$ . We further classified outlier

$\alpha$  parameter estimates for a locus based on whether the median of the posterior sample was positive or negative. Positive estimates of  $\alpha$  mean there is a greater probability of *A. americanus* ancestry in individuals at the locus relative to their hybrid index, whereas negative estimates of  $\alpha$  mean there is a greater probability of *A. terrestris* ancestry.

### 3.6 Genetic differentiation and Introgression

To test for a relationship between patterns of introgression and genetic divergence, we used *VCFTools* to calculate the Weir and Cockerham (1984)  $F_{ST}$  between each species using only the samples inferred through the *STRUCTURE* analysis to have >95% ancestry for one species under the model with a  $K$  of two (Danecek et al., 2011). The Weir and Cockerham  $F_{ST}$  is calculated per-site and we calculated the per-site  $F_{ST}$  for the same sites as those used in the *BGC* analysis. To determine if patterns of introgression are correlated with population differentiation, we calculated Pearson's correlation coefficients between  $F_{ST}$  and the  $\alpha$  and  $\beta$  parameters using *SciPy* with the default p-value calculation. To calculate the correlation coefficient, we used the absolute value of the median of the posterior sample for the  $\alpha$  parameter and the median of the posterior sample for the  $\beta$  parameter. To further test for a relationship between population differentiation and  $\alpha$ , we binned loci as positive alpha outliers, negative alpha outliers, and non-outliers. To test for differences in values of  $F_{ST}$  among these three groups of loci, we used a Kruskal-Wallis test using *SciPy* v1.10.1 (Virtanen et al., 2020). To determine which groups differ significantly from each other, we used pairwise Mann-Whitney U tests with Bonferroni correction using *scikit-posthocs* ([github.com/maximtrp/scikit-posthocs](https://github.com/maximtrp/scikit-posthocs)).

## 4 Results

### 4.1 Sampling and Data Processing

We prepared reduced-representation sequencing libraries from 173 samples collected for this study (Table S1) and 19 samples available from existing collections (Table S2)). The *Stacks* pipeline assembled reads into 432,336 loci with a mean length of 253.31 bp.

Prior to filtering the mean coverage per sample was 32X. After filtering loci missing from greater than 5% of samples, filtering sites with minor allele counts less than 3, filtering individuals with greater than 90% missing loci, and randomly sampling a single SNP from each locus, 1194 sites remained and 43 samples were excluded from further analyses leaving a total of 149. For the included samples, 56 had been identified as most closely resembling *A. americanus* and 93 had been identified as most closely resembling *A. terrestris*.

## 4.2 Genetic Clustering & Ancestry Proportions

A visual inspection of the *STRUCTURE* results shows that each run with same value for  $K$  converged on very similar results (Fig. S1). The *STRUCTURE* model with the largest  $\Delta K$  was the model with a  $K$  of two (Fig. S2). Furthermore, individuals are inferred as having ancestry derived largely from only two ancestral groups even for  $K$  values of three and four. For these values of  $K$ , only a small amount of ancestry is attributed to the third or fourth ancestral groups for any individual sample (Fig. S3). Using a 95% estimated ancestry proportion as a cutoff for considering individuals to have pure ancestry, 36 samples were classified as pure *A. americanus*, 75 as pure *A. terrestris*, and 38 as being admixed. The proportions of admixture among the samples shows a clear gradient between 0 and 1 which is consistent with many individuals being the product of advanced-generation hybrids beyond the  $F_1$  generation. The transition of admixture proportions from one species to the other with distance from the locations of pure individuals with proportions closest to 0.5 being found in the center of this transition (Fig. 1).

## 4.3 Patterns of Introgression

Visualization of the MCMC output with trace plots and histograms of each parameter indicated that each of the five chains run in *BGC* quickly converged on the same parameter space. We conservatively discarded the first 10% of samples as burnin. The median of the posterior sample for cline center parameter  $\alpha$  ranged from -0.525-0.494

across loci. The cline shape parameter  $\beta$  was less variable and ranged from -0.158-0.220 across loci. We identified 16 loci with "excess ancestry" for the  $\alpha$  parameter relative to the genome wide average; i.e., the 90% HDPI does not cover 0. Of these, the median of the posterior sample for 5 of these loci was negative and for 11 loci was positive. Negative values represent a greater probability of *A. americanus* ancestry at a locus relative to the individual's hybrid index whereas positive values represent a greater probability of *A. terrestris* ancestry. We identified 116 loci as being "outliers" for the  $\alpha$  parameter; i.e., they are statistically unlikely relative to the genome-wide distribution of locus-specific introgression. Of these, the median of the posterior sample for 24 of these loci was negative and for 92 loci it was positive (Fig. 2). All 16 of the loci identified as having "excess ancestry" for the  $\alpha$  parameter relative to the genome-wide average were also identified as "outliers" relative to the genome-wide distribution of locus-specific introgression. We did not classify any loci as having "excess ancestry" or as being "outliers" with respect to the  $\beta$  parameter.

#### 4.4 Genomic Differentiation

Genetic differentiation between *A. americanus* and *A. terrestris* was highly variable among loci (Fig. 3). Locus-specific  $F_{ST}$  between non-admixed *A. americanus* and *A. terrestris* had a mean of 0.07.  $F_{ST}$  values for 249 loci were 0. Only a single locus had fixed differences between species with an  $F_{ST}$  of 1.0. There is little apparent relationship between  $\alpha$  or  $\beta$  and  $F_{ST}$  except at the highest  $\alpha$  and  $\beta$  estimates which have  $F_{ST}$  estimates well above zero (Fig. 4). The Pearson correlation test estimates a weak correlation between  $\alpha$  and  $F_{ST}$  ( $r=0.29$ ,  $p=1.62e-23$ ) and between  $\beta$  and  $F_{ST}$  ( $r=0.32$ ,  $p = 8.28 \times 10^{-30}$ ). The result of the Kruskal-Wallis test are consistent with there being significant differences between the  $F_{ST}$  values of loci with outlier  $\alpha$  estimates and non-outlier  $\alpha$  estimates on average ( $H = 183.66$ ,  $p = 1.32 \times 10^{-40}$ ) (Fig. 3). The results of the post hoc pairwise Mann-Whitney tests are consistent with both categories of loci with outlier  $\alpha$  estimates having greater  $F_{ST}$  values on average than the non-outlier estimates of  $\alpha$ . The difference between non-outlier loci and loci with greater probability of *A. americanus* ancestry was

slightly higher ( $U = 88495$ , Bonferroni corrected  $p = 8.15 \times 10^{-38}$ ) than the difference between non-outlier loci and loci with greater *A. terrestris* ancestry ( $U = 19519$ , Bonferroni corrected  $p = 2.45 \times 10^{-5}$ ). Loci with greater probability of *A. americanus* ancestry had greater  $F_{ST}$  on average than loci with greater probability of *A. terrestris* ancestry ( $U1741$ , Bonferroni corrected  $P = 4.32e - 05$ ).

## 5 Discussion

### 5.1 Evidence for ongoing hybridization

With the genome-wide sequence data obtained in this study, we find evidence of substantial gene flow across the hybrid zone of these two species. The *STRUCTURE* analysis inferred 38 out of 149 samples as having a proportion of ancestry of at least 5% of sites attributable to admixture (Fig. 1). The admixture proportions inferred in the *STRUCTURE* analysis range from 0.05-0.5 which is consistent with hybrids being viable, fertile, and capable of backcrossing over multiple generations (Fig. 1) (Slager et al., 2020). When backcrossing occurs over multiple generations in combination with migration of hybrid progeny and selection against introgressing alleles, a cline will form across the hybrid zone with introgressing alleles becoming more uncommon with distance from the cline edge (Barton & Hewitt, 1985). The results of the *STRUCTURE* analysis are largely consistent with this. Inferred admixture coefficients are highest at the center of the hybrid zone and decrease and approach zero with distance from the center (Fig. 1).

Admixed samples were located quite far from the center of the hybrid zone. In fact samples with greater than 5% admixture proportions are located all the way at the Northeastern and Southwestern edges of the sampling area. The width of a hybrid zone is a product of the strength of selection for or against introgression and the average dispersal distance of individuals within their reproductive lifespan (Barton & Hewitt, 1985). Breden (1987) estimated that 27% of individual *A. fowleri* breed at non-natal breeding ponds with some dispersing more than 2 km. Female *A. americanus* have been shown to migrate more than 1 km between breeding sites and post-breeding locations

(Forester et al., 2006). Invasive cane toads (*Rhinella marina*) in Australia are estimated to have expanded their range at a rate of 10-15 km per year shortly after their introduction although this rate slowed with time (Urban et al., 2008). The presence of samples with little to no admixture in close proximity to toads with high proportions of admixture shows that dispersal patterns may have an important role in shaping the patterns of introgression in this hybrid zone. Individuals would be expected to appear more like their neighbors if dispersal rates and distances were very low and homogeneous. It is also likely that this hybrid zone may be more appropriately described as a mosaic hybrid zone rather than a more simple tension zone (Harrison, 1986). However, the sampling for this study is too sparse and irregular to definitively test this. Another possibility is that some of this inferred admixture is the result of a statistical artifact or due to error. *STRUCTURE* can only model admixture and not ancestral polymorphism which would be classified by the program as admixture (Pritchard et al., 2000). Some reassurance is provided by the result of the PCA which is largely consistent with the *STRUCTURE* results although it is possible that they could be affected by the same bias or error introduced in data collection and processing (Fig. 1).

The tension zone model of hybrid zones predicts that location of hybrid zones centers will be dependent on the effects of selection along with population density and natural dispersal barriers (Barton, 1979). The *STRUCTURE* results show that in two areas, there is a clear transition from samples with primarily *A. americanus* ancestry to samples with primarily *A. terrestris* ancestry corresponding with the locations of streams and rivers. In the Northern part of the sampling area, transitions occur at the Coosa River and at Waxahatchee Creek (Fig. 1). In the Southern part, they occur at Sougahatchee Creek (Fig. 1). Clearly these are not impassable boundaries as there has been introgression beyond them. However, they likely reduce dispersal and as a result the center of the hybrid zone is caught in this location as described by Barton (1979).

## 5.2 Variability of introgression

There are two primary parameters of interest in a genomic cline model that can be interpreted in the evolutionary context of hybrid zones. The  $\alpha$  parameter specifies the center of the cline and is dependent on the increase or decrease in the probability of locus-specific ancestry from one of the parental populations. The  $\beta$  parameter specifies the rate of change in probability of ancestry along the genome-wide admixture gradient. Extreme estimates of these parameters may be associated with loci that cause reproductive incompatibility between hybridizing species. The Bayesian genomic cline analysis of the genome-wide data in this study yielded extreme estimates for  $\alpha$  at some sites. Sites were classified as having extreme values in two ways. First, sites could be classified as having excess ancestry if the HDPI of  $\alpha$  or  $\beta$  does not cover zero and is therefore extreme relative to the genome-wide average of cline parameter estimates. Second, sites could be classified as being outliers if they are extreme relative to the genome-wide distribution of locus-specific effects under the cline model. A greater number of sites qualified as outliers for estimates of  $\alpha$  than qualified as having excess ancestry. There were 116 loci classified as outliers which make up 9.7% of the total number of sites. Of those, 16 were also classified as having excess ancestry making up 1.3% of all sites. This difference is consistent with other studies using both simulated and empirical data which typically find more outlier loci than excess ancestry loci (Gompert & Buerkle, 2012). Both of these methods can produce false positives as these extreme values can be produced solely by genetic drift rather than by selection (Gompert & Buerkle, 2012). So not all sites with extreme estimates will be associated with incompatibility loci. The false positive rate is exacerbated when there are many loci with small effects on compatibility. However, these sites should be enriched for loci associated with modest to strong reproductive incompatibility and thus provide an upper estimate of the number of sites that are associated with these modest to strong barriers to gene flow (Gompert & Buerkle, 2012).

None of the estimates for  $\beta$  were classified as either outliers or as having excess ancestry. Simulations have demonstrated that the  $\alpha$  parameter is more impacted by selection against hybrid genotypes than the  $\beta$  parameter (Gompert, Lucas, et al., 2012).

Other studies have also found no extreme estimates of  $\beta$  (Gompert, Lucas, et al., 2012; Nikolakis et al., 2022). One possible interpretation of the absence of extreme values of  $\beta$  is that selection is only strong enough to have a significant impact on  $\alpha$  but it is not strong enough to have a large impact on  $\beta$ . Unlike for  $\alpha$ , there is not a strong relationship between locally positive selection favoring introgressed genotypes and  $\beta$  (Gompert, Lucas, et al., 2012). Therefore, some of the extreme values for  $\alpha$  could be due to adaptive introgression which does not have much impact on estimates of  $\beta$ . This is plausible given the large extent of introgression we observed. Some of which is potentially due to adaptive introgression. It has been shown that there is a negative relationship between  $\beta$  and dispersal rate (Gompert, Lucas, et al., 2012). It is therefore also plausible that high dispersal rates, rather than selection is the cause of lower  $\beta$  values that do not reach the threshold to qualify as extreme.

Of the 9.7% of sites that qualified as  $\alpha$  outliers, a substantially larger proportion had positive values which represent greater *A. americanus* ancestry than expected at those sites in admixed individuals. Negative  $\alpha$  estimates represent a greater probability of *A. terrestris* ancestry at a site within admixed individuals. Sites with positive outlier estimates for  $\alpha$  made up 7.7% of all sites whereas those with negative outlier estimates made up just 2%. This asymmetry suggests that introgression flows more in the direction of *A. americanus* than it does in the direction of *A. terrestris*. This result is consistent with a pattern evident upon visual inspection of the mapped *STRUCTURE* results. Samples collected from sites adjacent to sites with admixed samples appear to have a greater proportion of *A. terrestris* ancestry than *A. americanus* ancestry (Fig. 1). Taken together, these observations suggest that introgression at this hybrid zone is asymmetric (Yang et al., 2020). Asymmetries in introgression can arise for multiple reasons. There could be differences in mate choice which make females of one species more selective than females of the other (Baldassarre et al., 2014). There can also be species differences in dispersal tendencies. Reciprocal-cross differences in reproductive isolation, termed Darwin's Corollary, are very common (Turelli & Moyle, 2007). If one of the sexes is more prone to dispersal, introgression will flow more freely in one direction than it would in

the other. It is possible that this observation is just an artifact of sampling. Particularly if this is a highly mosaic hybrid zone. However, many more samples with primarily *A. terrestris* ancestry were collected than samples with primarily *A. americanus* ancestry.

### 5.3 Relationship between introgression and differentiation

Patterns of genetic differentiation and genomic introgression between *A. americanus* and *A. terrestris* are consistent with the hypothesis that regions of the genome experiencing divergent selection also affect hybrid fitness. As predicted, there is a positive association between locus-specific estimates of  $F_{ST}$  and both the absolute value of the  $\alpha$  and the  $\beta$  parameter estimates. Although this correlation supports the hypothesis that introgression outliers are linked to loci under selection, the association is only a modest one. Despite this, it is notable all of the outlier  $\alpha$  estimates as well as the highest  $\beta$  estimates have  $F_{ST}$  estimates well above zero. Whereas sites with lower  $\alpha$  and  $\beta$  estimates span the entire range from zero to one. This is consistent with expectations of secondary contact where not all loci that have undergone genomic divergence will necessarily result in reproductive isolation. A tighter coupling of divergence and resistance to gene flow would be expected under a scenario of divergence with gene flow.

### 5.4 Conclusion

In conclusion, the genome-wide sequence data analysis conducted in this study has provided compelling evidence of significant gene flow across the hybrid zone of *A. americanus* and *A. terrestris*. The *STRUCTURE* analysis reveals that a substantial number of samples have ancestry proportions attributable to hybridization. These findings suggest that hybrids are not only viable and fertile but also capable of backcrossing over multiple generations. Furthermore, the spatial distribution of admixture coefficients suggests the formation of a cline, with the highest levels of admixture at the hybrid zone's center gradually diminishing with distance. Patterns in the distribution of admixture coefficients suggest a potentially important role for rivers as a partial barrier to dispersal. We found a weak relationship between loci with limited introgression and the degree

of genetic divergence, measured with  $F_{ST}$ . This study demonstrates that introgression between *A. americanus* and *A. terrestris* is ongoing and can serve as a guide for future studies which could leverage quantitative measures of prezygotic isolation such as calls or spawning period, reference genomes, or crossing experiments paired with cutting edge genomic tools to shed light on the process of speciation.

## 5.5 Data Availability

All raw sequence reads have been deposited in the NCBI Short Read Archive under BioProject PRJNA1108277. Sample accessions are listed in Table S1 and Table S1. Scripts used for analysis are available at [github.com/kerrycobb/toad-evolution](https://github.com/kerrycobb/toad-evolution).

## 6 Acknowledgments

We thank Holden Smith and Charlotte Benedict for assistance in the field and laboratory. We also thank the University of Texas at El Paso Biodiversity Collections for the gifting of one sample used in this study. This work was completed in part with resources provided by the Auburn University Easley Cluster. This article is contribution number 964 of the Auburn University Museum of Natural History.

## References

Baldassarre, D. T., White, T. A., Karubian, J., & Webster, M. S. (2014). GENOMIC AND MORPHOLOGICAL ANALYSIS OF A SEMIPERMEABLE AVIAN HYBRID ZONE SUGGESTS ASYMMETRICAL INTROGRESSION OF A SEXUAL SIGNAL. *Evolution*, 68(9), 2644–2657. <https://doi.org/10.1111/evo.12457>

Barton, N. H. (1979). The dynamics of hybrid zones. *Heredity*, 43(3), 341–359. <https://doi.org/10.1038/hdy.1979.87>

Barton, N. H., & Hewitt, G. M. (1985). Analysis of Hybrid Zones. *Annual Review*, 16, 113–148.

Bayona-Vásquez, N. J., Glenn, T. C., Kieran, T. J., Pierson, T. W., Hoffberg, S. L., Scott, P. A., Bentley, K. E., Finger, J. W., Louha, S., Troendle, N., Diaz-Jaimes, P., Mauricio, R., & Faircloth, B. C. (2019). Adapterama III: Quadruple-indexed, double/triple-enzyme RADseq libraries (2RAD/3RAD). *PeerJ*, 7, e7724. <https://doi.org/10.7717/peerj.7724>

Blackman, B. (2016). Speciation Genes. *Encyclopedia of Evolutionary Biology* (pp. 166–175). Elsevier. <https://doi.org/10.1016/B978-0-12-800049-6.00066-4>

Blair, W. F. (1963). Intragroup genetic compatibility in the *Bufo americanus* species group of toads. *The Texas Journal of Science*, 13, 15–34.

Blair, W. F. (1972). *Evolution in the genus Bufo*. University of Texas Press.

Breden, F. (1987). The Effect of Post-Metamorphic Dispersal on the Population Genetic Structure of Fowler's Toad, *Bufo woodhousei fowleri*. *Copeia*, 1987(2), 386–395. <https://doi.org/10.2307/1445775>

Butlin, R., Debelle, A., Kerth, C., Snook, R. R., Beukeboom, L. W., RF, C. C., Diao, W., Maan, M. E., Paolucci, S., Weissing, F. J., et al. (2011). What do we need to know about speciation? *Trends in ecology & evolution*, 27(1), 27–39.

Crocroft, R. B., & Ryan, M. J. (1995). Patterns of advertisement call evolution in toads and chorus frogs. *Animal Behaviour*, 49(2), 283–303. <https://doi.org/10.1006/anbe.1995.0043>

Colliard, C., Sicilia, A., Turrisi, G. F., Arculeo, M., Perrin, N., & Stöck, M. (2010). Strong reproductive barriers in a narrow hybrid zone of West-Mediterranean green toads (*Bufo viridissubgroup*) with Plio-Pleistocene divergence. *BMC Evolutionary Biology*, 10(1), 232. <https://doi.org/10.1186/1471-2148-10-232>

Coyne, J. A., & Orr, H. A. (2004). *Speciation*. Sinauer Associates.

Danecek, P., Auton, A., Abecasis, G., Albers, C. A., Banks, E., DePristo, M. A., Handlaker, R. E., Lunter, G., Marth, G. T., Sherry, S. T., McVean, G., Durbin, R., & 1000 Genomes Project Analysis Group. (2011). The variant call format and VCFtools. *Bioinformatics*, 27(15), 2156–2158. <https://doi.org/10.1093/bioinformatics/btr330>

Đorđević, S., & Simović, A. (2014). STRANGE AFFECTION: MALE BUFO BUFO (ANURA: BUFONIDAE) PASSIONATELY EMBRACING A BULGE OF MUD. *Ecologica Montenegrina*, 1(1), 15–17. <https://doi.org/10.37828/em.2014.1.4>

Evanno, G., Regnaut, S., & Goudet, J. (2005). Detecting the number of clusters of individuals using the software structure: A simulation study. *Molecular Ecology*, 14(8), 2611–2620. <https://doi.org/10.1111/j.1365-294X.2005.02553.x>

Forester, D. C., Snodgrass, J. W., Marsalek, K., & Lanham, Z. (2006). Post-Breeding Dispersal and Summer Home Range of Female American Toads (*Bufo americanus*). *Northeastern Naturalist*, 13(1), 59–72. [https://doi.org/10.1656/1092-6194\(2006\)13\[59:PDASHR\]2.0.CO;2](https://doi.org/10.1656/1092-6194(2006)13[59:PDASHR]2.0.CO;2)

Francis, R. M. (2017). POPHELPER: An R package and web app to analyse and visualize population structure. *Molecular Ecology Resources*, 17(1), 27–32. <https://doi.org/10.1111/1755-0998.12509>

Gompert, Z., & Buerkle, C. A. (2012). Bgc: Software for Bayesian estimation of genomic clines. *Molecular Ecology Resources*, 12(6), 1168–1176. <https://doi.org/10.1111/1755-0998.12009.x>

Gompert, Z., & Buerkle, C. A. (2011). Bayesian estimation of genomic clines: BAYESIAN GENOMIC CLINES. *Molecular Ecology*, 20(10), 2111–2127. <https://doi.org/10.1111/j.1365-294X.2011.05074.x>

Gompert, Z., Lucas, L. K., Nice, C. C., Fordyce, J. A., Forister, M. L., & Buerkle, C. A. (2012). GENOMIC REGIONS WITH A HISTORY OF DIVERGENT SELECTION AFFECT FITNESS OF HYBRIDS BETWEEN TWO BUTTERFLY SPECIES: GENOMICS OF SPECIATION. *Evolution*, 66(7), 2167–2181. <https://doi.org/10.1111/j.1558-5646.2012.01587.x>

Gompert, Z., Mandeville, E. G., & Buerkle, C. A. (2017). Analysis of Population Genomic Data from Hybrid Zones. *Annual Review of Ecology, Evolution, and Systematics*, 48(1), 207–229. <https://doi.org/10.1146/annurev-ecolsys-110316-022652>

Gompert, Z., Parchman, T. L., & Buerkle, C. A. (2012). Genomics of isolation in hybrids. *Philosophical Transactions of the Royal Society B: Biological Sciences*, 367(1587), 439–450. <https://doi.org/10.1098/rstb.2011.0196>

Green, D. M. (1983). Allozyme Variation through a Clinal Hybrid Zone between the Toads *Bufo americanus* and *B. hemiophrys* in Southeastern Manitoba. *Herpetologica*, 39(1), 28–40.

Green, D. M. (1996). The bounds of species: Hybridization in the *Bufo americanus* group of North American toads. *Israel Journal of Zoology*, 42, 95–109.

Harrison, R. G. (1986). Pattern and process in a narrow hybrid zone. *Heredity*, 56(3), 337–349. <https://doi.org/10.1038/hdy.1986.55>

Hedrick, P. W. (2013). Adaptive introgression in animals: Examples and comparison to new mutation and standing variation as sources of adaptive variation. *Molecular Ecology*, 22(18), 4606–4618. <https://doi.org/10.1111/mec.12415>

Hunter, J. D. (2007). Matplotlib: A 2D Graphics Environment. *Computing in Science & Engineering*, 9(3), 90–95. <https://doi.org/10.1109/MCSE.2007.55>

Jahner, J. P., Parchman, T. L., & Matocq, M. D. (2021). Multigenerational backcrossing and introgression between two woodrat species at an abrupt ecological transition. *Molecular Ecology*, 30(17), 4245–4258. <https://doi.org/10.1111/mec.16056>

Jombart, T. (2008). Adegenet : A R package for the multivariate analysis of genetic markers. *Bioinformatics*, 24(11), 1403–1405. <https://doi.org/10.1093/bioinformatics/btn129>

Larson, E. L., Andrés, J. A., Bogdanowicz, S. M., & Harrison, R. G. (2013). DIFFERENTIAL INTROGRESSION IN A MOSAIC HYBRID ZONE REVEALS CANDIDATE BARRIER GENES. *Evolution*, 67(12), 3653–3661. <https://doi.org/10.1111/evo.12205>

Mallet, J. (2005). Hybridization as an invasion of the genome. *Trends in Ecology & Evolution*, 20(5), 229–237. <https://doi.org/10.1016/j.tree.2005.02.010>

Mallet, J. (2008). Hybridization, ecological races and the nature of species: Empirical evidence for the ease of speciation. *Philosophical Transactions of the Royal Society*

*B: Biological Sciences*, 363(1506), 2971–2986. <https://doi.org/10.1098/rstb.2008.0081>

Malone, J. H., & Fontenot, B. E. (2008). Patterns of Reproductive Isolation in Toads (R. DeSalle, Ed.). *PLoS ONE*, 3(12), e3900. <https://doi.org/10.1371/journal.pone.0003900>

Miller, C. J. J., & Matute, D. R. (2016). The Effect of Temperature on Drosophila Hybrid Fitness. *G3: Genes/Genomes/Genetics*, 7(2), 377–385. <https://doi.org/10.1534/g3.116.034926>

Moran, B. M., Payne, C., Langdon, Q., Powell, D. L., Brandvain, Y., & Schumer, M. (2021). The genomic consequences of hybridization (P. J. Wittkopp, Ed.). *eLife*, 10, e69016. <https://doi.org/10.7554/eLife.69016>

Mount, R. H. (1975). *The Reptiles and Amphibians of Alabama*. The University of Alabama Press.

Nikolakis, Z. L., Schield, D. R., Westfall, A. K., Perry, B. W., Ivey, K. N., Orton, R. W., Hales, N. R., Adams, R. H., Meik, J. M., Parker, J. M., Smith, C. F., Gompert, Z., Mackessy, S. P., & Castoe, T. A. (2022). Evidence that genomic incompatibilities and other multilocus processes impact hybrid fitness in a rattlesnake hybrid zone. *Evolution*, 76(11), 2513–2530. <https://doi.org/10.1111/evo.14612>

Nosil, P., Funk, D. J., & Ortiz-Barrientos, D. (2009). Divergent selection and heterogeneous genomic divergence. *Molecular Ecology*, 18(3), 375–402. <https://doi.org/10.1111/j.1365-294X.2008.03946.x>

Nosil, P., & Schlüter, D. (2011). The genes underlying the process of speciation. *Trends in Ecology & Evolution*, 26(4), 160–167. <https://doi.org/10.1016/j.tree.2011.01.001>

Parchman, T. L., Gompert, Z., Braun, M. J., Brumfield, R. T., McDonald, D. B., Uy, J. a. C., Zhang, G., Jarvis, E. D., Schlinger, B. A., & Buerkle, C. A. (2013). The genomic consequences of adaptive divergence and reproductive isolation between species of manakins. *Molecular Ecology*, 22(12), 3304–3317. <https://doi.org/10.1111/mec.12201>

Powell, R., Conant, R., & Collins, J. T. (2016). *A Field Guide to Reptiles & Amphibians: Eastern and Central North America* (4th ed.). Houghton Mifflin Harcourt.

Pritchard, J. K., Stephens, M., & Donnelly, P. (2000). Inference of Population Structure Using Multilocus Genotype Data. *Genetics*, 155(2), 945–959. <https://doi.org/10.1093/genetics/155.2.945>

Rieseberg, L. H., Whitton, J., & Gardner, K. (1999). Hybrid zones and the genetic architecture of a barrier to gene flow between two sunflower species. *Genetics*, 152(2), 713–727.

Rochette, N. C., Rivera-Colón, A. G., & Catchen, J. M. (2019). Stacks 2: Analytical methods for paired-end sequencing improve RADseq-based population genomics. *Molecular Ecology*, 28(21), 4737–4754. <https://doi.org/10.1111/mec.15253>

Servedio, M. R., & Noor, M. A. (2003). The Role of Reinforcement in Speciation: Theory and Data. *Annual Review of Ecology, Evolution, and Systematics*, 34(1), 339–364. <https://doi.org/10.1146/annurev.ecolsys.34.011802.132412>

Shankman, D., & Hart, J. L. (2007). The Fall Line: A Physiographic-Forest Vegetation Boundary. *Geographical Review*, 97(4), 502–519. <https://doi.org/10.1111/j.1931-0846.2007.tb00409.x>

Slager, D. L., Epperly, K. L., Ha, R. R., Rohwer, S., Wood, C., Van Hemert, C., & Klicka, J. (2020). Cryptic and extensive hybridization between ancient lineages of American crows. *Molecular Ecology*, 29(5), 956–969. <https://doi.org/10.1111/mec.15377>

Taylor, E. B., Boughman, J. W., Groenenboom, M., Sniatynski, M., Schluter, D., & Gow, J. L. (2006). Speciation in reverse: Morphological and genetic evidence of the collapse of a three-spined stickleback (*Gasterosteus aculeatus*) species pair. *Molecular Ecology*, 15(2), 343–355. <https://doi.org/10.1111/j.1365-294X.2005.02794.x>

Turelli, M., & Moyle, L. C. (2007). Asymmetric Postmating Isolation: Darwin's Corollary to Haldane's Rule. *Genetics*, 176(2), 1059–1088. <https://doi.org/10.1534/genetics.106.065979>

Urban, M. C., Phillips, B. L., Skelly, D. K., & Shine, R. (2008). A Toad More Traveled: The Heterogeneous Invasion Dynamics of Cane Toads in Australia. *The American Naturalist*, 171(3), E134–E148. <https://doi.org/10.1086/527494>

Van Riemsdijk, I., Arntzen, J. W., Bucciarelli, G. M., McCartney-Melstad, E., Rafajlović, M., Scott, P. A., Toffelmier, E., Shaffer, H. B., & Wielstra, B. (2023). Two transects reveal remarkable variation in gene flow on opposite ends of a European toad hybrid zone. *Heredity*. <https://doi.org/10.1038/s41437-023-00617-6>

Virtanen, P., Gommers, R., Oliphant, T. E., Haberland, M., Reddy, T., Cournapeau, D., Burovski, E., Peterson, P., Weckesser, W., Bright, J., van der Walt, S. J., Brett, M., Wilson, J., Millman, K. J., Mayorov, N., Nelson, A. R. J., Jones, E., Kern, R., Larson, E., ... SciPy 1.0 Contributors. (2020). SciPy 1.0: Fundamental algorithms for scientific computing in python. *Nature Methods*, 17, 261–272. <https://doi.org/10.1038/s41592-019-0686-2>

Weatherby, C. A. (1982). INTROGRESSION BETWEEN THE AMERICAN TOAD, *BUFO AMERICANUS*, AND THE SOUTHERN TOAD, *B. TERRESTRIS*, IN ALABAMA.

Weir, B. S., & Cockerham, C. C. (1984). Estimating F-Statistics for the Analysis of Population Structure. *Evolution*, 38(6), 1358–1370. <https://doi.org/10.2307/2408641>

Wolf, J. B. W., & Ellegren, H. (2017). Making sense of genomic islands of differentiation in light of speciation. *Nature Reviews Genetics*, 18(2), 87–100. <https://doi.org/10.1038/nrg.2016.133>

Wu, C.-I. (2001). The genic view of the process of speciation. *Journal of Evolutionary Biology*, 14(6), 851–865. <https://doi.org/10.1046/j.1420-9101.2001.00335.x>

Yang, W., Feiner, N., Laakkonen, H., Sacchi, R., Zuffi, M. A. L., Scali, S., While, G. M., & Uller, T. (2020). Spatial variation in gene flow across a hybrid zone reveals causes of reproductive isolation and asymmetric introgression in wall lizards. *Evolution*, 74(7), 1289–1300. <https://doi.org/10.1111/evo.14001>

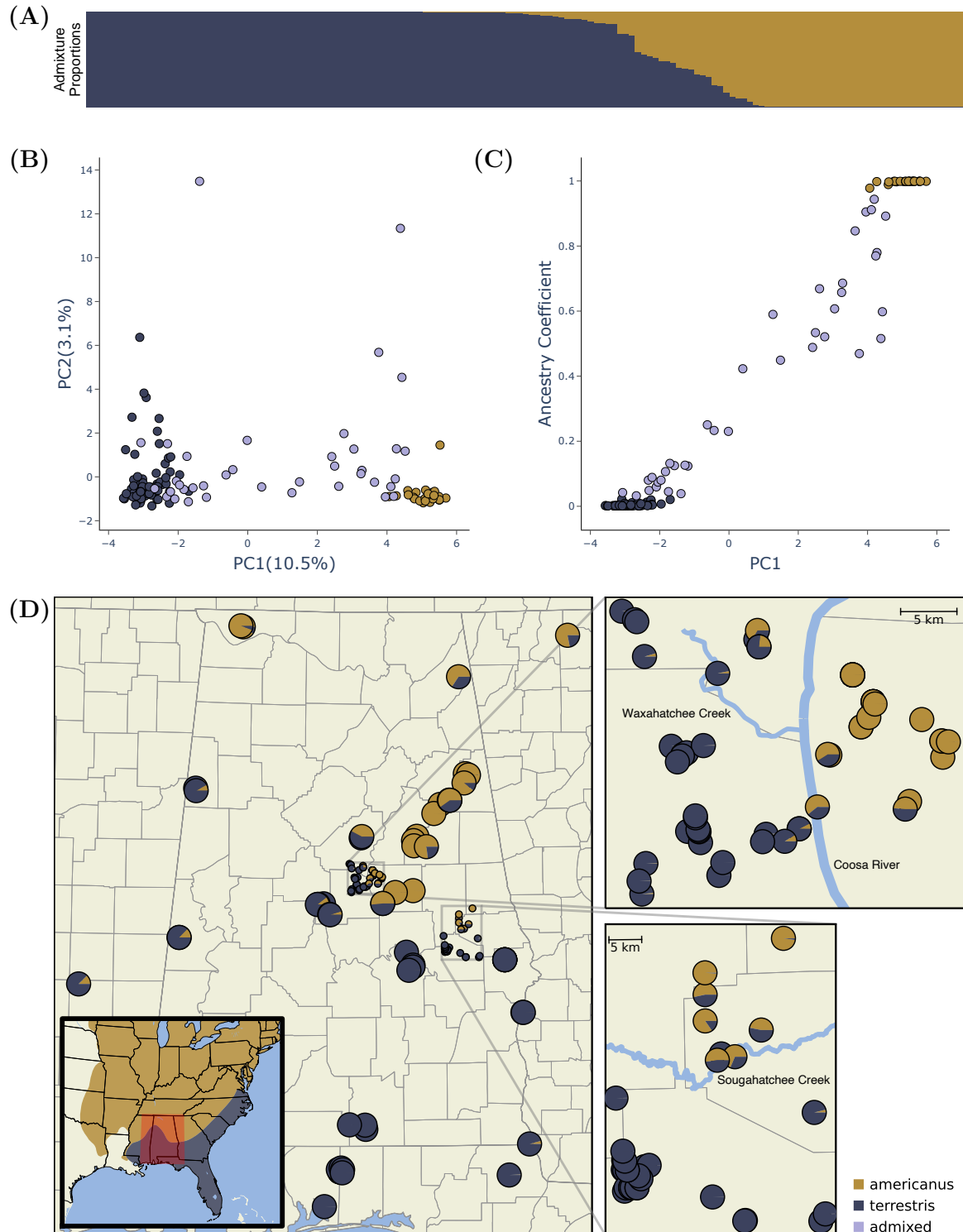


Figure 1. Genetic evidence of hybridization between *A. americanus* and *A. terrestris*. (A) Bar plot with the ancestry coefficients estimated with *STRUCTURE*. (B) Summary of population genetic structure based on the principal component axes one (PC1) and two (PC2). These axes explain 10.5% (PC1) and 3.1% (PC2) of the genetic variation among individuals. (C) Relationship between the first principal component axis and the admixture proportions estimated with *STRUCTURE*. (D) Sample map showing the sampling location and estimated ancestry coefficients of each sample. The inset map shows the approximate ranges of each species and the study area highlighted in red. Figure created using *POPHelper* (Francis, 2017) and *Matplotlib* (Hunter, 2007)

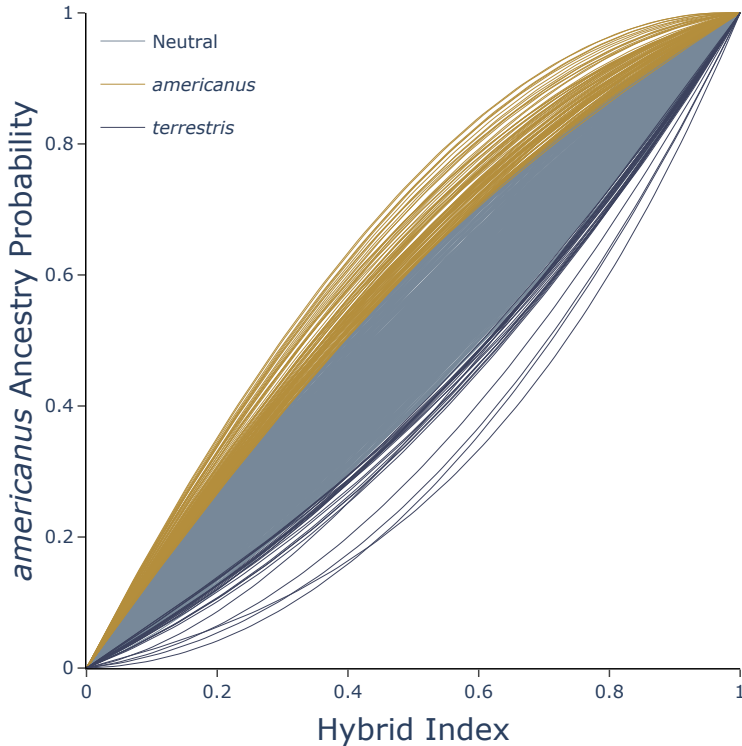


Figure 2. Shape of genomic clines estimated for each locus with *BGC*. Outliers are highlighted with yellow for loci that have greater *A. americanus* ancestry than expected and blue if loci have greater *A. terrestris* ancestry than expected.

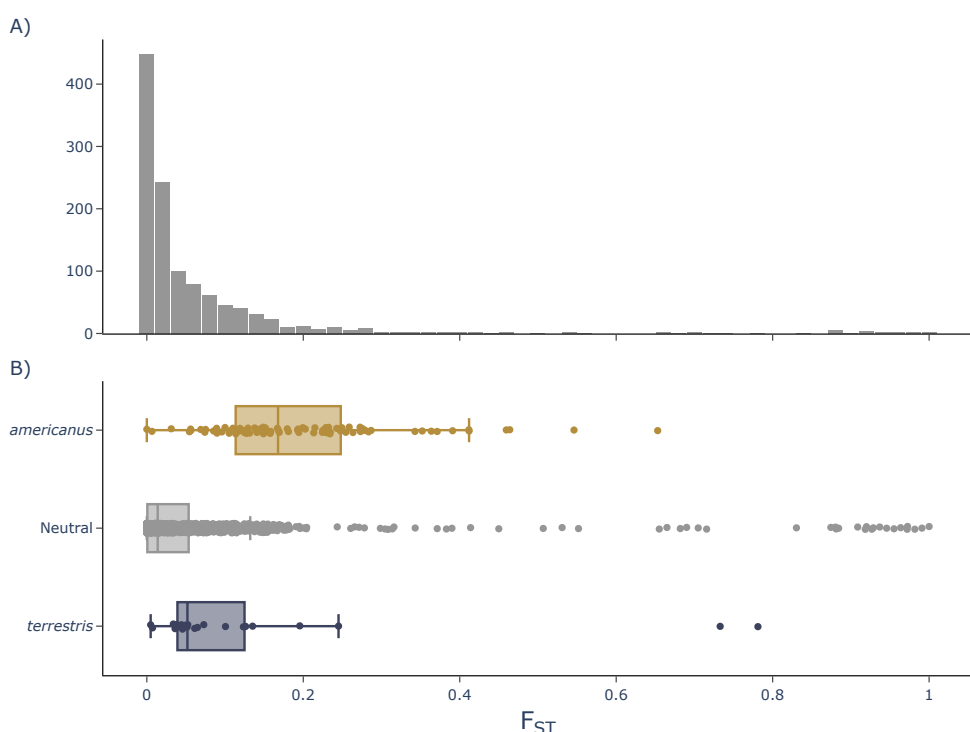


Figure 3. A) Distribution of per site  $F_{ST}$  estimates. B) Box plots showing the distribution and mean of  $F_{ST}$  for three categories of  $\alpha$  estimates: outliers with greater than expected *A. americanus* ancestry (gold), outliers with greater than expected *A. terrestris* ancestry (violet), and non-outliers (gray).

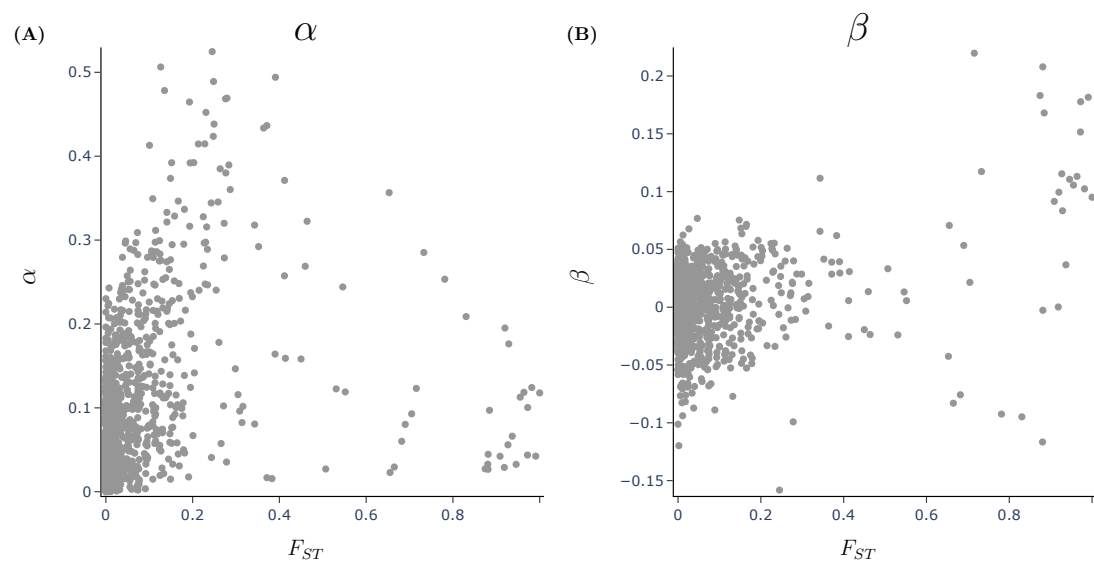


Figure 4. Relationship between genetic divergence measured with Weir and Cockerham, 1984  $F_{ST}$  and BGC cline parameters A)  $\alpha$  and B)  $\beta$ .

## Supplementary Material

Title: Genomic Evidence for Hybridization and Introgression in a North American Toad (*Anaxyrus*) Hybrid Zone

Authors: Kerry A. Cobb (Corresponding author: [cobbkerry@gmail.com](mailto:cobbkerry@gmail.com))<sup>1</sup> and Jamie R. Oaks<sup>2</sup>

<sup>1</sup>Department of Biological Sciences, Mississippi State University, Mississippi State, MS 39762

<sup>2</sup>Department of Biological Sciences & Museum of Natural History, Auburn University, 101 Rouse Life Sciences Building, Auburn, Alabama 36849

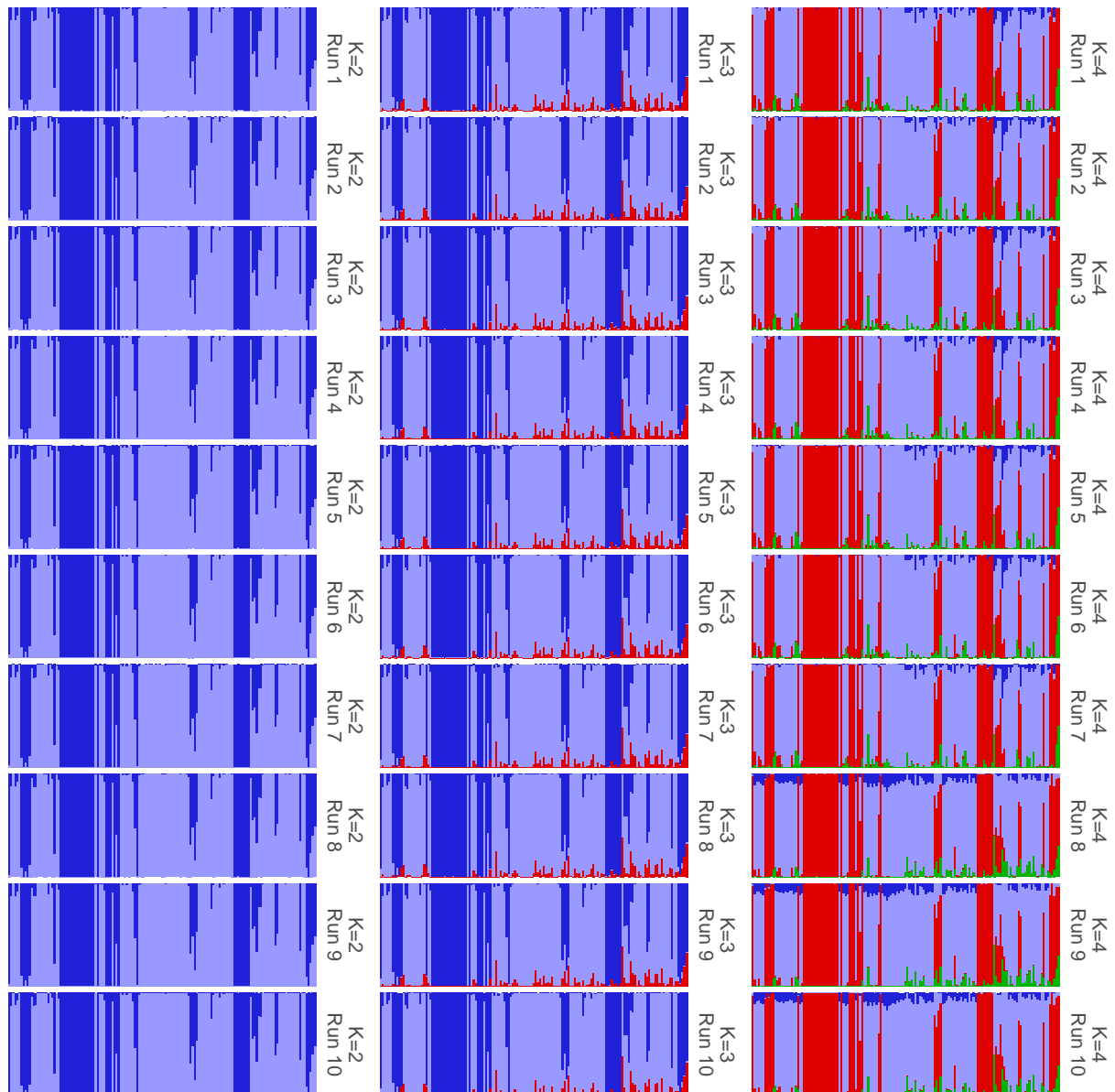


Figure SS1. Results of each independent *STRUCTURE* run (rows) for each value of  $K$  (columns) showing convergence among runs with the same value for  $K$ . Plot was created with *POPHelper* (Francis, 2017).

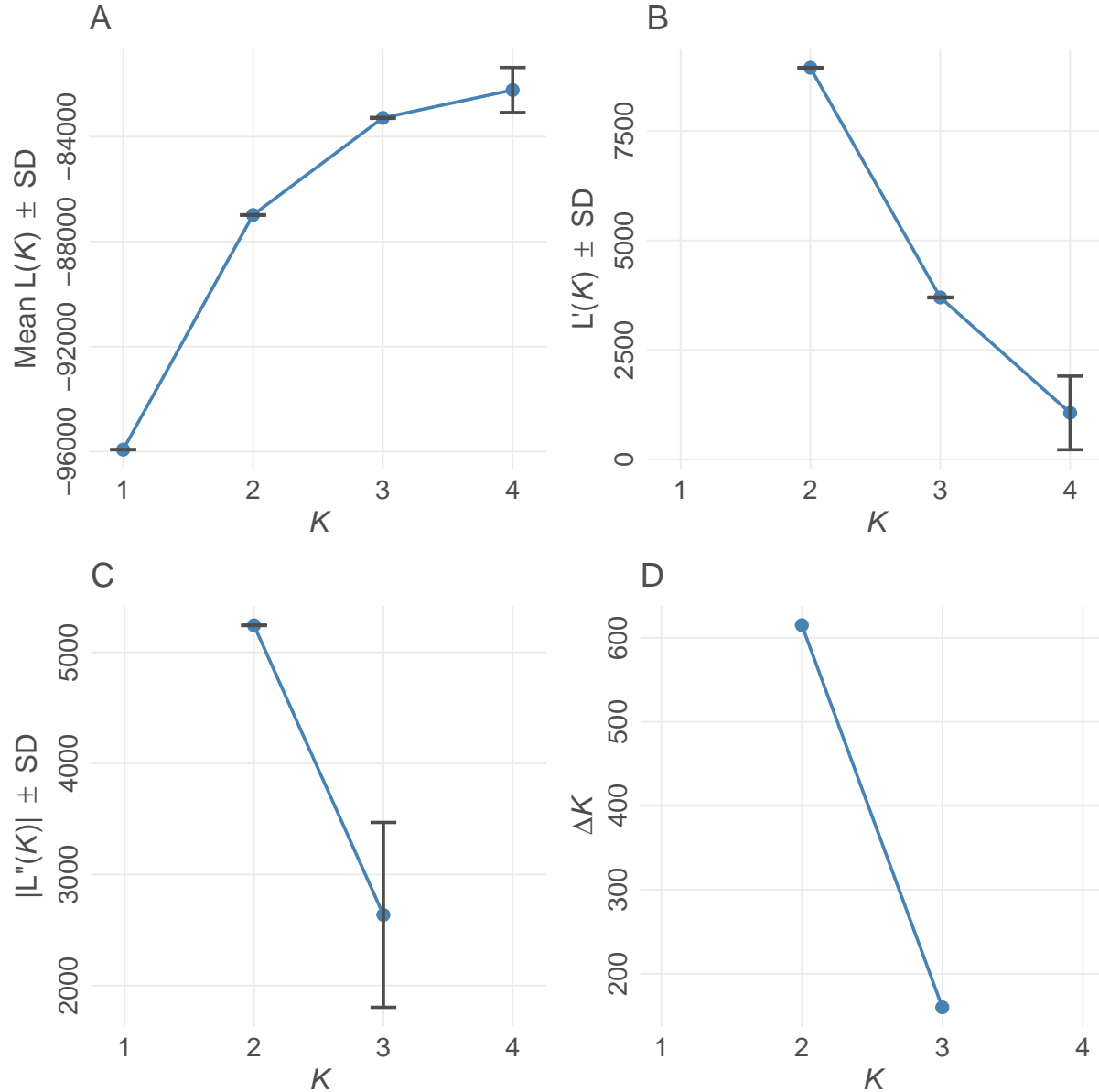


Figure SS2. Evanno method for optimal value for  $K$  in *STRUCTURE* (Evanno et al., 2005).  $K$  refers to the number of populations for each of the different *STRUCTURE* models examined. (A) Mean estimated  $\ln$  probability of data over 10 iterations for each value of  $K \pm SD$ . (B) Rate of change of the likelihood distribution (mean  $\pm SD$ ) (C) Absolute values of the second order rate of change of the likelihood distribution (mean  $\pm SD$ ) (D)  $\Delta K$ . The modal value of this distribution is considered the true value of  $K$  for the data. Plot created using *POPHELP* (Francis, 2017).

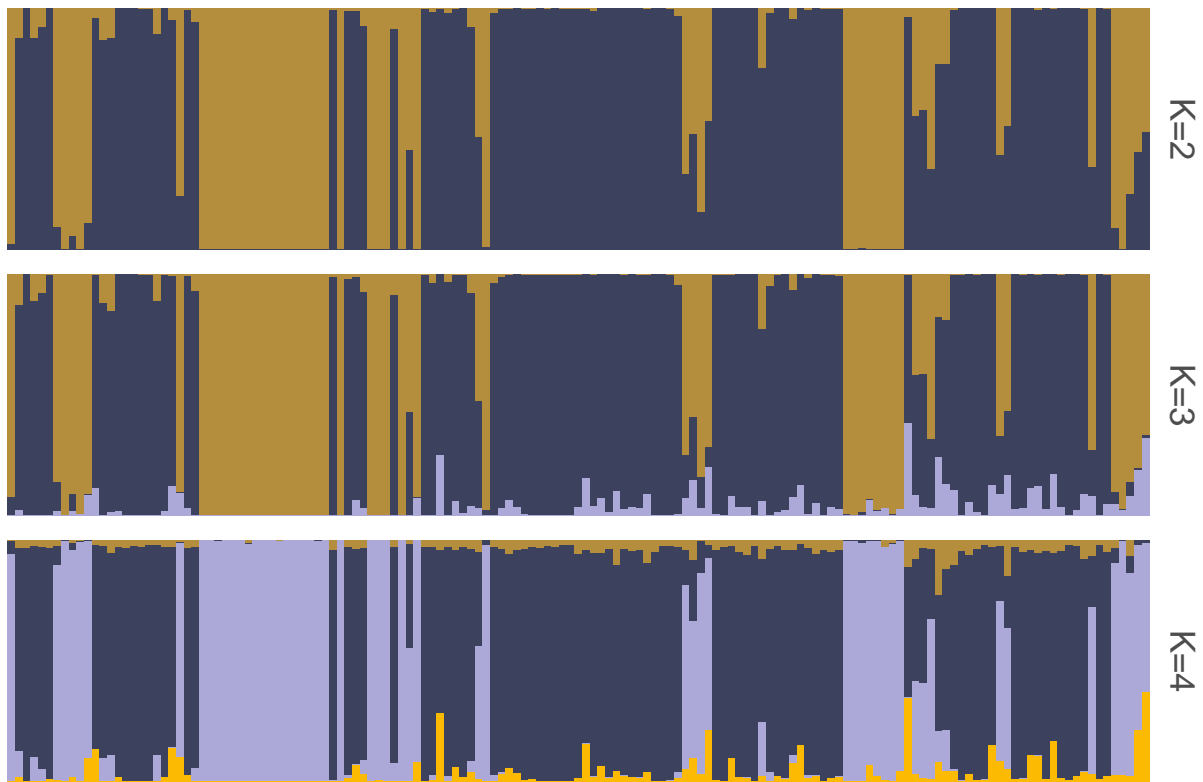


Figure SS3. Summarized *STRUCTURE* results for each value of  $K$ . Ancestry proportions shown are the mean of ancestry proportions across all iterations. Summarization and plotting done using *POPHELPER* (Francis, 2017).

Table S1. – Samples collected for this study

ID	Voucher	SRA	Species	Passed Filter	Latitude	Longitude
046	AUHT 7962	SRR28909866	<i>A. terrestris</i>	X	30.54819	-86.93067
047	AUHT 7974	SRR28909865	<i>A. terrestris</i>	X	32.81470	-86.93968
048	AUHT 7975	SRR28909864	<i>A. terrestris</i>	X	32.81094	-86.98967
049	AUHT 7976	SRR28909863	<i>A. terrestris</i>	X	32.80985	-86.99795
050	AUHT 7978	SRR28909862	<i>A. terrestris</i>		32.82406	-86.99314
051	AUHT 7979	SRR28909860	<i>A. terrestris</i>		32.82406	-86.99314
052	AUHT 7980	SRR28909859	<i>A. terrestris</i>		32.80450	-87.03078
053	AUHT 7981	SRR28909858	<i>A. terrestris</i>		32.76703	-87.07073
054	AUHT 7982	SRR28909857	<i>A. terrestris</i>		32.76592	-87.07184
055	AUHT 7983	SRR28909856	<i>A. terrestris</i>		32.78932	-86.90850
056	AUHT 7984	SRR28909855	<i>A. terrestris</i>	X	32.73575	-86.88149
057	AUHT 7985	SRR28909854	<i>A. terrestris</i>	X	32.73291	-86.87707
058	AUHT 7986	SRR28909853	<i>A. terrestris</i>		32.74822	-86.79806
059	AUHT 7987	SRR28909852	<i>A. terrestris</i>		32.78742	-86.75847
060	AUHT 7988	SRR28909851	<i>A. terrestris</i>		32.78044	-86.73877
069	AUHT 8006	SRR28909793	<i>A. americanus</i>	X	34.79963	-84.57678
070	AUHT 8007	SRR28909792	<i>A. terrestris</i>		32.43478	-85.64630
071	AUHT 8010	SRR28909790	<i>A. terrestris</i>	X	30.77430	-85.22690
072	AUHT 8011	SRR28909789	<i>A. terrestris</i>	X	32.94778	-86.63224
073	AUHT 8012	SRR28909788	<i>A. terrestris</i>		32.94970	-86.52687
074	AUHT 8013	SRR28909787	<i>A. terrestris</i>		32.94970	-86.52687
075	AUHT 8014	SRR28909786	<i>A. americanus</i>	X	33.00267	-86.38960
076	AUHT 8015	SRR28909785	<i>A. americanus</i>		33.01205	-86.47872
077	AUHT 8016	SRR28909784	<i>A. americanus</i>		33.04456	-86.45547
078	AUHT 8017	SRR28909783	<i>A. americanus</i>	X	33.04456	-86.45547
079	AUHT 8018	SRR28909782	<i>A. americanus</i>	X	33.04456	-86.45547

Continued on next page

Table S1 – continued from previous page

ID	Voucher	SRA	Species	Passed Filter	Latitude	Longitude
080	AUHT 8019	SRR28909781	<i>A. americanus</i>	X	33.04456	-86.45547
081	AUHT 8020	SRR28909779	<i>A. americanus</i>	X	33.04456	-86.45547
082	AUHT 8021	SRR28909778	<i>A. americanus</i>		33.04456	-86.45547
083	AUHT 8022	SRR28909964	<i>A. americanus</i>	X	33.04456	-86.45547
084	AUHT 8023	SRR28909963	<i>A. americanus</i>	X	33.01484	-86.39040
085	AUHT 8025	SRR28909962	<i>A. americanus</i>	X	33.01484	-86.39040
086	AUHT 8026	SRR28909961	<i>A. americanus</i>	X	33.06472	-86.47496
087	AUHT 8027	SRR28909960	<i>A. americanus</i>	X	33.06472	-86.47496
088	AUHT 8028	SRR28909959	<i>A. americanus</i>		33.06472	-86.47496
089	AUHT 8029	SRR28909958	<i>A. americanus</i>	X	33.06472	-86.47496
090	AUHT 8030	SRR28909957	<i>A. americanus</i>	X	33.06472	-86.47496
091	AUHT 8031	SRR28909955	<i>A. americanus</i>	X	33.06472	-86.47496
092	AUHT 8032	SRR28909954	<i>A. americanus</i>	X	33.06472	-86.47496
093	AUHT 8033	SRR28909953	<i>A. americanus</i>	X	33.06472	-86.47496
094	AUHT 8034	SRR28909952	<i>A. americanus</i>	X	33.02572	-86.46711
095	AUHT 8035	SRR28909951	<i>A. americanus</i>	X	33.02572	-86.46711
096	AUHT 8036	SRR28909950	<i>A. terrestris</i>	X	32.92374	-86.67199
097	AUHT 8037	SRR28909949	<i>A. americanus</i>	X	33.03283	-86.45975
098	AUHT 8038	SRR28909948	<i>A. terrestris</i>	X	32.94544	-86.55777
099	AUHT 8039	SRR28909947	<i>A. terrestris</i>	X	32.94947	-86.52630
100	AUHT 8040	SRR28909946	<i>A. terrestris</i>	X	32.94947	-86.52630
101	AUHT 8041	SRR28910057	<i>A. americanus</i>	X	33.04278	-86.45377
102	AUHT 8042	SRR28910056	<i>A. americanus</i>	X	33.00464	-86.49692
103	AUHT 8043	SRR28910055	<i>A. americanus</i>	X	33.01416	-86.38417
104	AUHT 8044	SRR28910054	<i>A. terrestris</i>	X	32.94013	-86.54004
105	AUHT 8045	SRR28910053	<i>A. terrestris</i>		32.94173	-86.55787

Continued on next page

Table S1 – continued from previous page

ID	Voucher	SRA	Species	Passed Filter	Latitude	Longitude
106	AUHT 8046	SRR28910052	<i>A. americanus</i>	X	33.03099	-86.40941
107	AUHT 8047	SRR28910051	<i>A. americanus</i>	X	33.00518	-86.49895
108	AUHT 8048	SRR28910050	<i>A. terrestris</i>		32.95011	-86.53723
109	AUHT 8049	SRR28910049	<i>A. americanus</i>		33.00528	-86.38897
110	AUHT 8050	SRR28910048	<i>A. americanus</i>		33.01617	-86.40318
111	AUHT 8051	SRR28910046	<i>A. americanus</i>		32.98218	-86.40488
112	AUHT 8052	SRR28910045	<i>A. americanus</i>	X	32.96964	-86.42137
113	AUHT 8053	SRR28910044	<i>A. terrestris</i>		32.97146	-86.52901
114	AUHT 8057	SRR28910043	<i>A. terrestris</i>	X	32.44120	-85.65386
115	AUHT 8058	SRR28910042	<i>A. terrestris</i>		32.85411	-86.76619
116	AUHT 8059	SRR28910041	<i>A. terrestris</i>	X	32.90084	-86.67587
117	AUHT 8060	SRR28910040	<i>A. terrestris</i>	X	32.91060	-86.67850
118	AUHT 8061	SRR28910039	<i>A. terrestris</i>		32.91715	-86.68208
119	AUHT 8062	SRR28910038	<i>A. terrestris</i>		32.92717	-86.67407
120	AUHT 8063	SRR28910037	<i>A. terrestris</i>		32.97159	-86.62516
121	AUHT 8064	SRR28910011	<i>A. terrestris</i>		33.00585	-86.63703
122	AUHT 8065	SRR28910010	<i>A. terrestris</i>		33.00797	-86.64210
123	AUHT 8066	SRR28910009	<i>A. terrestris</i>		33.00818	-86.64333
124	AUHT 8067	SRR28910008	<i>A. terrestris</i>		33.01508	-86.64937
125	AUHT 8068	SRR28910007	<i>A. terrestris</i>		33.02034	-86.66651
126	AUHT 8069	SRR28910006	<i>A. terrestris</i>	X	33.01163	-86.64759
127	AUHT 8070	SRR28910005	<i>A. terrestris</i>	X	33.00537	-86.63652
128	AUHT 8071	SRR28910004	<i>A. terrestris</i>	X	33.00644	-86.63368
129	AUHT 8072	SRR28910003	<i>A. terrestris</i>	X	33.00673	-86.63316
131	AUHT 8074	SRR28910000	<i>A. americanus</i>	X	32.70224	-85.66196
132	AUHT 8075	SRR28909999	<i>A. americanus</i>	X	32.73042	-85.66173

Continued on next page

Table S1 – continued from previous page

ID	Voucher	SRA	Species	Passed Filter	Latitude	Longitude
133	AUHT 8076	SRR28909998	<i>A. terrestris</i>	X	32.62553	-85.63684
134	AUHT 8077	SRR28909997	<i>A. terrestris</i>	X	32.41032	-85.60107
135	AUHT 8078	SRR28909996	<i>A. terrestris</i>	X	32.57011	-85.80888
136	AUHT 8079	SRR28909995	<i>A. terrestris</i>	X	32.47773	-85.79824
137	AUHT 8080	SRR28909994	<i>A. terrestris</i>	X	32.47707	-85.79577
138	AUHT 8081	SRR28909993	<i>A. terrestris</i>	X	32.48128	-85.76354
139	AUHT 8082	SRR28909992	<i>A. terrestris</i>	X	32.48291	-85.75622
140	AUHT 8083	SRR28909991	<i>A. terrestris</i>	X	32.45001	-85.79652
141	AUHT 8084	SRR28909989	<i>A. terrestris</i>	X	32.45420	-85.79408
142	AUHT 8085	SRR28909945	<i>A. terrestris</i>	X	32.45449	-85.78664
143	AUHT 8086	SRR28909944	<i>A. terrestris</i>	X	32.45449	-85.78664
144	AUHT 8087	SRR28909943	<i>A. terrestris</i>	X	32.45451	-85.78416
145	AUHT 8088	SRR28909942	<i>A. terrestris</i>	X	32.45423	-85.77634
146	AUHT 8089	SRR28909941	<i>A. terrestris</i>	X	32.45423	-85.77634
147	AUHT 8090	SRR28909940	<i>A. terrestris</i>	X	32.46574	-85.76977
148	AUHT 8091	SRR28909939	<i>A. terrestris</i>	X	32.46961	-85.77369
149	AUHT 8092	SRR28909938	<i>A. terrestris</i>	X	32.47709	-85.79175
151	AUHT 8094	SRR28909935	<i>A. terrestris</i>	X	32.47709	-85.79175
152	AUHT 8095	SRR28909934	<i>A. terrestris</i>	X	32.49000	-85.79741
153	AUHT 8096	SRR28909933	<i>A. terrestris</i>	X	32.40809	-85.47857
154	AUHT 8097	SRR28909932	<i>A. terrestris</i>	X	32.41744	-85.47117
155	AUHT 8098	SRR28909931	<i>A. terrestris</i>	X	32.35417	-86.09838
156	AUHT 8099	SRR28909930	<i>A. terrestris</i>	X	32.33994	-86.09946
157	AUHT 8100	SRR28909929	<i>A. terrestris</i>	X	32.31562	-86.13789
160	AUHT 8103	SRR28909926	<i>A. terrestris</i>	X	33.06620	-86.60328
161	AUHT 8108	SRR28909924	<i>A. americanus</i>	X	32.62171	-85.61467

Continued on next page

Table S1 – continued from previous page

ID	Voucher	SRA	Species	Passed Filter	Latitude	Longitude
162	AUHT 8109	SRR28909923	<i>A. americanus</i>	X	32.61751	-85.64335
165	AUHT 8112	SRR28909848	<i>A. americanus</i>	X	32.66836	-85.66233
166	AUHT 8113	SRR28909847	<i>A. americanus</i>	X	32.65571	-85.57134
170	AUHT 8117	SRR28909843	<i>A. terrestris</i>	X	32.38644	-85.23561
171	AUHT 8118	SRR28909841	<i>A. terrestris</i>	X	32.38579	-85.23565
172	AUHT 8119	SRR28909840	<i>A. terrestris</i>	X	32.38579	-85.23565
173	AUHT 8120	SRR28909839	<i>A. terrestris</i>	X	32.38579	-85.23565
174	AUHT 8121	SRR28909838	<i>A. terrestris</i>	X	32.38579	-85.23565
176	AUHT 8123	SRR28909836	<i>A. americanus</i>		32.64548	-85.55135
177	AUHT 8124	SRR28909835	<i>A. terrestris</i>	X	32.40976	-85.60208
178	AUHT 8125	SRR28909834	<i>A. terrestris</i>	X	33.09152	-86.56686
179	AUHT 8126	SRR28909833	<i>A. terrestris</i>	X	33.11298	-86.69434
180	AUHT 8127	SRR28909832	<i>A. terrestris</i>	X	33.10659	-86.68228
181	AUHT 8128	SRR28909830	<i>A. terrestris</i>	X	33.10509	-86.68014
182	AUHT 8129	SRR28909829	<i>A. terrestris</i>	X	33.07896	-86.67286
183	AUHT 8130	SRR28909828	<i>A. terrestris</i>	X	32.93933	-86.62008
184	AUHT 8131	SRR28909827	<i>A. terrestris</i>	X	32.94745	-86.62146
185	AUHT 8132	SRR28909826	<i>A. terrestris</i>	X	32.94829	-86.62190
186	AUHT 8133	SRR28909988	<i>A. terrestris</i>	X	32.94929	-86.62241
187	AUHT 8134	SRR28909987	<i>A. terrestris</i>		32.95077	-86.62306
188	AUHT 8135	SRR28909986	<i>A. terrestris</i>	X	32.95794	-86.62477
189	AUHT 8136	SRR28909985	<i>A. terrestris</i>	X	32.95940	-86.62489
209	AUHT 8141	SRR28910034	<i>A. terrestris</i>	X	32.54852	-85.48692
210	AUHT 8142	SRR28910033	<i>A. americanus</i>	X	33.30759	-86.58201
211	AUHT 8143	SRR28910031	<i>A. americanus</i>	X	33.31685	-86.57596
212	AUHT 8144	SRR28910030	<i>A. americanus</i>	X	33.09829	-86.56529

Continued on next page

Table S1 – continued from previous page

ID	Voucher	SRA	Species	Passed Filter	Latitude	Longitude
213	AUHT 8145	SRR28910029	<i>A. terrestris</i>	X	33.08600	-86.56394
214	AUHT 8146	SRR28910028	<i>A. terrestris</i>	X	33.08600	-86.56394
215	AUHT 8147	SRR28910027	<i>A. terrestris</i>		33.01464	-86.60995
216	AUHT 8148	SRR28910026	<i>A. terrestris</i>	X	33.01208	-86.61707
217	AUHT 8149	SRR28910025	<i>A. terrestris</i>	X	33.00435	-86.63710
218	AUHT 8150	SRR28910024	<i>A. terrestris</i>	X	32.99991	-86.64181
219	AUHT 8151	SRR28910023	<i>A. terrestris</i>		32.99605	-86.64526
220	AUHT 8152	SRR28910022	<i>A. terrestris</i>		33.01346	-86.60960
221	AUHT 8153	SRR28910020	<i>A. terrestris</i>	X	32.91470	-86.60270
222	AUHT 8154	SRR28910019	<i>A. terrestris</i>	X	32.92432	-86.59895
223	AUHT 8155	SRR28910018	<i>A. terrestris</i>	X	32.93987	-86.56113
224	AUHT 8156	SRR28910017	<i>A. americanus</i>	X	32.96579	-86.50892
225	AUHT 8157	SRR28910016	<i>A. americanus</i>	X	32.96389	-86.42549
226	AUHT 8159	SRR28910015	<i>A. terrestris</i>		32.53362	-85.79839
227	AUHT 8160	SRR28910014	<i>A. terrestris</i>	X	32.48869	-85.79555
228	AUHT 8161	SRR28910013	<i>A. terrestris</i>	X	32.50159	-85.79860
230	AUHT 8166	SRR28909920	<i>A. terrestris</i>	X	30.80933	-86.77686
231	AUHT 8167	SRR28909918	<i>A. terrestris</i>	X	30.80922	-86.78994
232	AUHT 8169	SRR28909917	<i>A. terrestris</i>	X	30.80922	-86.78994
233	AUHT 8170	SRR28909916	<i>A. terrestris</i>	X	30.80922	-86.78994
234	AUHT 8172	SRR28909915	<i>A. terrestris</i>	X	30.82632	-86.80258
235	AUHT 8173	SRR28909914	<i>A. terrestris</i>	X	30.83733	-86.77630
236	AUHT 8174	SRR28909913	<i>A. terrestris</i>	X	30.82433	-86.76284
237	AUHT 8175	SRR28909912	<i>A. terrestris</i>	X	30.80162	-86.76659
240	AUHT 8178	SRR28909909	<i>A. americanus</i>	X	34.50446	-85.63768
204	AUHT 8181	SRR28909967	<i>A. americanus</i>		34.21852	-87.36662

Continued on next page

Table S1 – continued from previous page

ID	Voucher	SRA	Species	Passed Filter	Latitude	Longitude
190	AUHT 8183	SRR28909984	<i>A. americanus</i>	X	33.55274	-85.82913
191	AUHT 8186	SRR28909982	<i>A. americanus</i>	X	33.48548	-85.88857
192	AUHT 8187	SRR28909981	<i>A. americanus</i>	X	33.31649	-86.05293
193	AUHT 8188	SRR28909980	<i>A. americanus</i>	X	33.28443	-86.08443
194	AUHT 8189	SRR28909979	<i>A. americanus</i>	X	33.24576	-86.08168
195	AUHT 8190	SRR28909978	<i>A. americanus</i>		32.91057	-86.09272
197	AUHT 8192	SRR28909976	<i>A. americanus</i>		32.95104	-86.14539
198	AUHT 8193	SRR28909975	<i>A. americanus</i>	X	32.89787	-86.26061
199	AUHT 8194	SRR28909974	<i>A. americanus</i>	X	32.81642	-86.38018
263	AUHT 8198	SRR28909811	<i>A. terrestris</i>	X	31.99016	-85.07046
262	AUHT 8200	SRR28909812	<i>A. terrestris</i>	X	31.99042	-85.07423
266	AUHT 8201	SRR28909808	<i>A. americanus</i>	X	33.23853	-85.96270
265	AUHT 8204	SRR28909809	<i>A. americanus</i>	X	33.58435	-85.74064
267	AUHT 8205	SRR28909807	<i>A. americanus</i>	X	33.58295	-85.73539
264	AUHT 8206	SRR28909810	<i>A. americanus</i>	X	33.58295	-85.73524
268	AUHT 8207	SRR28909806	<i>A. americanus</i>	X	32.81642	-86.38018
261	AUHT 8208	SRR28909813	<i>A. terrestris</i>		31.10783	-86.62247

Table S2. – Samples loaned from museum collections

ID	Voucher	SRA	Species	Passed Filter	Latitude	Longitude
001	AUHT 1975	SRR28910060	<i>A. americanus</i>	X	32.77356	-85.53325
002	AUHT 2456	SRR28910059	<i>A. terrestris</i>	X	32.19494	-89.23629
005	AUHT 2885	SRR28909872	<i>A. terrestris</i>	X	32.45090	-86.15934
007	AUHT 3419	SRR28909850	<i>A. terrestris</i>	X	33.67290	-88.16068
008	AUHT 3421	SRR28909791	<i>A. terrestris</i>	X	33.65420	-88.15580
009	AUHT 3428	SRR28909780	<i>A. terrestris</i>	X	31.12679	-86.54755
010	AUHT 3459	SRR28909956	<i>A. americanus</i>	X	34.88028	-87.71849
011	AUHT 3460	SRR28910058	<i>A. americanus</i>	X	33.78013	-85.58421
012	AUHT 3461	SRR28910047	<i>A. americanus</i>	X	34.88779	-87.74103
013	AUHT 3462	SRR28910012	<i>A. americanus</i>	X	33.77001	-85.55434
014	AUHT 3463	SRR28910001	<i>A. americanus</i>	X	33.71125	-85.59762
017	AUHT 3813	SRR28909925	<i>A. terrestris</i>		31.13854	-86.53906
018	AUHT 3833	SRR28909842	<i>A. terrestris</i>	X	31.00422	-85.03427
019	AUHT 3997	SRR28909831	<i>A. terrestris</i>	X	32.55607	-88.29975
020	AUHT 3998	SRR28909983	<i>A. terrestris</i>	X	32.55607	-88.29975
022	AUHT 5276	SRR28910032	<i>A. terrestris</i>		31.55613	-86.82514
023	AUHT 5277	SRR28910021	<i>A. terrestris</i>	X	31.15830	-86.55430
024	AUHT 5278	SRR28909919	<i>A. terrestris</i>	X	31.16105	-86.69868
273	UTEP 19947	SRR28909896	<i>A. terrestris</i>		31.22432	-88.77548